FINITE ELEMENT ANALYSIS FOR THE SEISMIC PERFORMANCE OF WALL-BEAM JOINT IN THICK WALL-THICK SLAB STRUCTURE

J. Wang [1], K. Kusunoki [2]

[1] *Ph.D. student, Earthquake Research Institute, The University of Tokyo, wangjiehui@eri.u-tokyo.ac.jp*
[2] *Professor, Earthquake Research Institute, The University of Tokyo, kusunoki@eri.u-tokyo.ac.jp*
…

Abstract

Since the 1923 Great Kanto earthquake, it has been observed that wall structures generally have better seismic performance compared to other more flexible and weaker frame buildings in Japan. Due to this, wall buildings are commonly used for Japanese residential buildings. One upcoming type of wall-building known as the "thick wall-thick slab" structure in which the structural system comprises solely of thick bearing walls and slabs, with part of the slab detailed as wide shallow beams. As the system provides larger interior open space compared to other wall buildings, it is gaining interest within Japan in both practice and research fields. However, a specific standard for the thick wall-thick slab wall structure has not been developed. Currently, the Architectural Institute of Japan (AIJ) is preparing a draft standard based on the existing equation for other wall and frame buildings. However, the accuracy and suitability of the equation need to be evaluated.

This study aims to address this need by performing finite element analyses on a joint of a thick wall-thick slab structure and to compare the strengths obtained with that predicted using the draft AIJ standard for this type of wall buildings. A numerical finite element model of a wall-beam joint was developed and calibrated against experimental results from a cyclic loading test performed at Yamaguchi University in 2016. A parametric study of the validated FEM model was performed to investigate the effect of wall aspect ratio, slab aspect ratio, and compressive axial load on the thick wall-thick slab system response.

When calibrating the FEM model, it was observed that the force-displacement relationship and damage/cracking to the joint numerical results matched well with the experimental results. From the consequent parametric study, it was found that: (i) the wall aspect ratio in the thick bearing wall influenced the lateral strength of the whole system, (ii) the slab aspect ratio did bring but not have a general influence on the overall system performance, and (iii) adding compressive axial load resulted in increase in the lateral flexural strength but had minor influence on the wall-beam joint. The results obtained from the draft AIJ standard equation used to predict the lateral flexural strength of the joint of thick wall-thick slab structure are compared against the numerical analysis results, where it was found that the lateral strength was sensitive to the aspect ratio of wall and slightly influenced by the aspect ratio of the portion of slab that not connected to the thick wall directly which was not yet considered in the draft equation to predict the lateral flexural strength of the joint, need to be modified according to experimental and numerical results. Based on these observations, evaluations to utilize the draft AIJ standard equation and recommendations for the next stage were proposed.

Keywords: thick wall-thick slab structure, seismic design code, experimental test, numerical modeling, parametric study

1. Introduction

Reinforced concrete wall structures (hereinafter WRC structure) are structures consisting of wall and beam elements monolithically constructed together and are widely used in low-rise residential apartment buildings in Japan. No column elements are used, and the beam usually has the same width as the wall. Over the past few decades, building damage investigations after earthquakes (e.g. the 1995 Hyogo-ken Nanbu Earthquake [1] and the 2016 Kumamoto earthquake [2]) had found that WRC structural systems had a good seismic performance.

Flat-plate-floor structural system is another type of structure which composes of slab and column elements. This type of structural framing system can offer several advantages, such as (i) easier construction, and (ii) larger interior space due to the absence of beam elements. However, since the shear failure is likely to occur at column-slab connections under lateral loading, the building would have small story shear capacities and thus this type of structural system is rarely used in seismically active countries such as Japan.

Based on these two structural systems, a new type called the thick-wall-thick-slab structure (TWTS), which consists of thick wall and thick slab elements had been developed. Interest in this system is increasing in Japan as a way to combine the advantage of high lateral stiffness and strength of WRC structures while providing more interior space like flat-plate-floor structures. The TWTS structural system consists of wall elements which are thicker than ordinary walls and provide the main resistance against lateral loading, and the slab element generally has the same depth as the wall's thickness and is only supported by the walls. However, a brittle fracture may still easily occur without any obvious deformation in the thick wall-thick slab joint.

In Japanese engineering practice, existing standards for flat-plate-floor RC structure and WRC structure established by the Architectural Institute of Japan (AIJ 2010 [3], AIJ 2015 [4]) are typically applied for frame building and wall building solution, respectively. These two aspects can be referred for developing a specific standard for the TWTS structural system. In order to accurately predict the seismic performance of the TWTS structure, the suitability of draft equations and provisions developed from past analytical studies and standards need to be evaluated.

In this paper, a finite-element model of a wall-slab joint element typically used in the TWTS structure is developed and validated against an experimental study conducted by Yamaguchi University in 2016 [5]. A parametric study was then performed to evaluate the accuracy of the proposed draft equation and the general performance of the thick wall-thick slab joint. The findings from this study would be used for developing and guiding the future research of TWTS structures.

2. Background

2.1 Draft equation

In engineering practice, the "strong column-weak beam" concept in which beams fail or form plastic hinges prior to the column to avoid progressive collapse is widely used designing of RC structures. This concept is also considered in TWTS structure to make sure the slab weaker than the strong wall to prevent the joint from collapse occurrence. In other words, the flexural capacity of the thick wall- thick slab joint is assumed to be controlled by the slab strength. According to the previous standards of flat-plate-floor [3] and WRC [4] structures, the flexural strength of slab element connected to the thick wall, $_sM_u$, can be calculated by Eq. (1).

$$_sM_u = 0.9\,\Sigma\big(a_t \cdot \sigma_y \cdot d\big) \tag{1}$$

where, a_t: cross-sectional area of flexural reinforcement in the slab, σ_y: nominal yield strength of flexural reinforcement, d: effective height of the slab.

2.2 Definition of equivalent beam

In the TWTS structure, a certain width of the floor slab near the wall (usually wider than the wall thickness), is detailed as if it were a wide and shallow beam element, and this beam portion is usually heavier reinforced than other portions of slab to strengthen the connection part with wall element. In addition, it is already defined as an "effective slab width model" in which a similar term called equivalent beam and part of the remainder

of the slab contribute to the overall lateral strength for flat-plate framing system by Laurel M et al. [6]. As for TWTS structure, when a wall-slab joint which is developed from the combination of the WRC structure and flat-plate structure is subjected to lateral loading, the existence of a similar term of "effective beam" can be expected and need to be confirmed.

3. Description of the specimen used in FEM analyses

The finite-element model of a wall-slab joint element typically used in this study is developed and validated against one specimen of an experimental study conducted by Yamaguchi University in 2016 [5]. In this experimental study, the specimen performed by Kawata et al. [5] is selected as the prototype of the FEM model and results were used to calibrate the FEM model. The specimen tested was a thick wall–thick slab connection and was constructed at 1/2-scale, and was tested under quasi-static lateral loading in the direction parallel to the wall's in-plane direction. The specimen's dimensions and details are shown in Fig.1 and Table 1. The loading setup used in this test is shown in Fig. 2, in which no constant vertical loading applied downward and cyclic lateral loading was applied by the horizontal actuator attached to the top of the wall. The entire cyclic loading process is controlled by the displacement on the top of the thick wall with 0.05%, 0.1%, 0.25%, 0.5%, 0.75%, 1%, 1.5%, 2%, 3% and 4% drift (measured from base support to top of the wall). Two cycles were applied for each drift level. The test results are presented together with FEM analysis results in section 4. The properties of concrete and rebar used in this specimen are summarized in Tables 2 and 3, respectively.
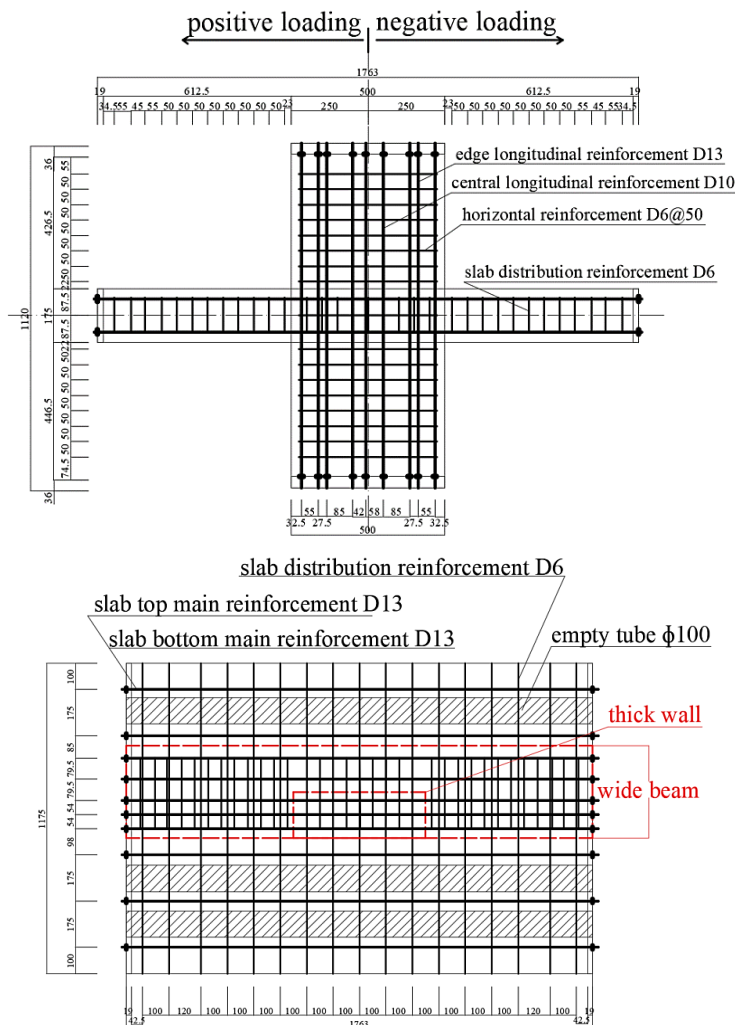

Fig. 1 – Dementions and details of the specimen tested by Kawata Y et al. [5] (units in mm)

Table 1 – Design detail of specimen [5]

| Element	Property	Value/Detail
Bearing wall	Length	500 mm
	Width	175 mm
	Height	1120 mm
	Main reinforcement	8-D13（edge）＋6-D10(center）
	Shear reinforcement	2-D6 @50
Slab beam	Length	1763 mm
	Width	350 mm
	Depth	175 mm
	Top/bottom reinforcement	5-D13
	Shear reinforcement	2-D6@50
slab	Length	1763 mm
	Width	1175 mm
	Depth	175 mm
	Reinforcement perpendicular to loading	5-D13
	Reinforcement parallel to loading	17-D16
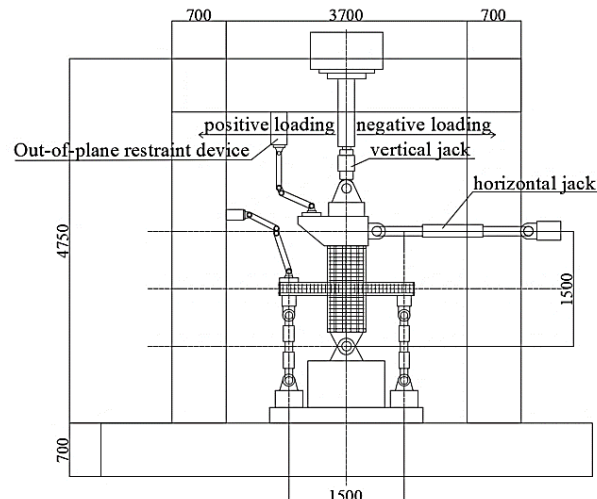
Fig. 2 – Loading equipment (units in mm) [5]

Table 2 – Properties of concrete [5]

Item	Compressive strength (MPa)	Young Modulus (×10⁴ MPa)	Tensile Strength (MPa)	Age (day)
concrete	27	2.52	2.19	46

4

2b-0070

Table 3 – Properties of reinforcing rebars [5]

Steel No.	Yielding Strength (MPa)	Yielding Strain	Tensile Strength (MPa)	Modulus of Elasticity (×10⁴ MPa)
D6	333	1850	492	1.82
D10	342	1795	495	1.91
D13	335	1783	490	1.88

4. Validation of the FEM model

4.1 General

A FEM model was created using the FINAL program [7], and FEM analyses were performed to simulate the behavior of thick wall-thick slab joint of TWTS structure under lateral loading. The configuration of the FEM model was identical to the specimen tested by Kawata et al. [5]. Hexahedron elements with 8 points for a single mesh and truss element with 2 points were used to model concrete and rebar, respectively. The model was divided into 7 different types due to different boundary condition, location, and reinforcement ratio as shown in Fig. 3 and Table 4. Support condition and loading setup was set identical with that in the experimental test.

4.2 Material models

Concrete type 1, 2, 5 and 6 (see Fig. 3) was modeled considering triaxial stress effects due to the presence of confining pressure and reinforcement. Therefore, Ottosen's four parameters model [8] with the coefficient of Hatanaka et al. in which the confining concrete pressure was considered to be less than 0.2 times the uniaxial compressive strength of concrete was adopted for the compressive fracture condition. Cover concrete (concrete type 3 and 4 from Fig. 3) was modeled considering biaxial stress effects due to there being no confinement effects, and thus the Kupfer-Gerstle model [9] was used for compressive fracture condition. For the tension stiffening model, the model proposed by Naganuma [10] shown in Fig. 4(a) was adopted for concrete type 1,2,4,5 and 6, including reinforcement ratio, concrete strength, and the compressive rigidity reduction rate effects, while the model developed by Izumo [11] with parameter C =1.0, shown in Fig. 4(b), was adopted for the cover concrete without reinforcement since the concrete cannot bear any tensile stresses after cracking. Then the following material properties were used for all concrete types, (i) the modified Ahmad model [8] showed in Fig.4(c) in which concrete was treated as Triaxial stress state, therefore, concrete confining pressure
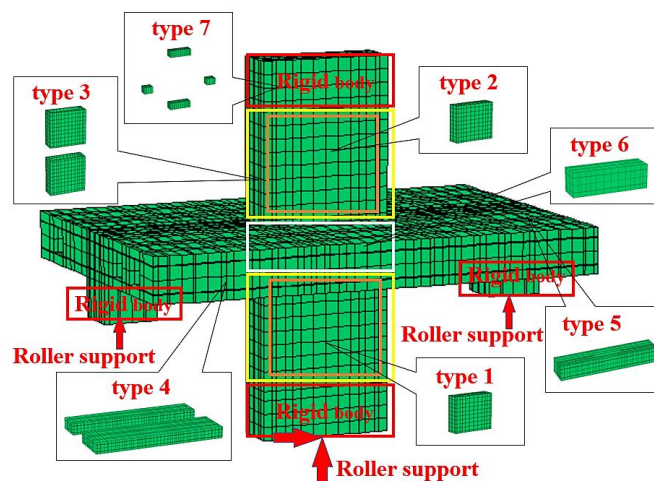

Fig. 3 – Decomposition detail of FEM model

5

Table 4 – Concrete types

Type	Location	Material condition
No.1	Central part of the lower part the wall	Confining pressure・reinforcement
No.2	Central part of the upper part the wall	Confining pressure・reinforcement
No.3	Cover concrete of wall	No confining pressure・reinforcement
No.4	Slab	No confining pressure・reinforcement
No.5	Wide Beam	Confining pressure・reinforcement
No.6	Connection part in slab and wall	Confining pressure・reinforcement
No.7	Loading part	Rigid body

and reinforcement ratio were both considered was adopted for the stress-strain relationship before compressive strength point, (ii) the method based on stress obtained from local strain at the crack local strain was adopted for judgment method of reinforcing rebar, (iii) the Naganuma model [8] in which the uniaxial compressive strength of concrete and the rebar axial compressive force both considered was used for compressive strength reduction after cracking, (iv) the curve model displayed in Fig.4(d) by Naganuma and Ohkubo [12] was applied here for the hysteresis relationship under cyclic loading for concrete since this behavior was close to the actual behavior.

A bilinear hysteretic model was assumed for the reinforcing bars as shown in Fig.5(a), where (i) the steel remains elastic till the yielding point is reached, (ii) strain hardening occurs with a post-yielding stiffness ratio of 0.001. Kinematic hardening, as shown in Fig. 5(b), was adopted for the rebar hardening law [13]. No bar slippage effects were considered for simplicity. More, the concrete and rebar were considered connected completely here.
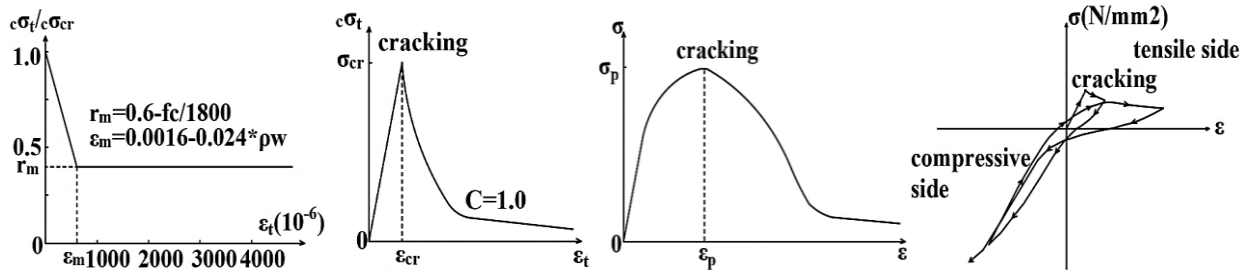

Fig. 4 – (a) Naganuma tension stiffening model [10], (b) Izumo model (C=1.0) [11]

(c) Modified Ahmad model [8], (d) curve model for hysteresis relationship under cyclic loading [12]
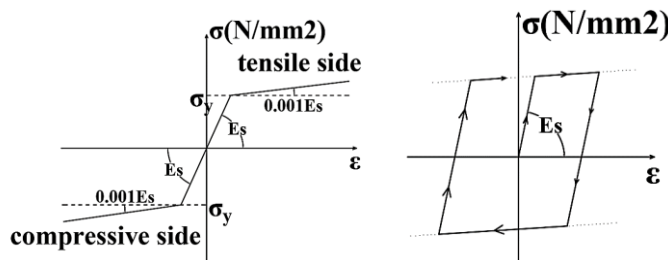

Fig. 5 – (a) Bilinear model, (b) Kinematic hardening law [13]

6

4.3 Comparison of test and FEM result

Fig. 6 shows the comparison of the force-displacement angle relationship between the experimental test and simulation results, where the blue and red color lines correspond to the experimental specimen response and FEM predictions, respectively. According to previous sections, the lateral flexural capacity of this wall-slab joint is controlled by the slab flexural strength. Assuming that only the "beam element" (the heavily reinforced portion of the slab) is considered to be effective to strength, the lateral flexural strength can be obtained from the slab flexural strength (see Fig.7) which is calculated using the Eq. (1) mentioned above. Fig. 8 illustrates the cracking pattern of the slab upper surface and wall surface at the end of test and FEM analysis, respectively.
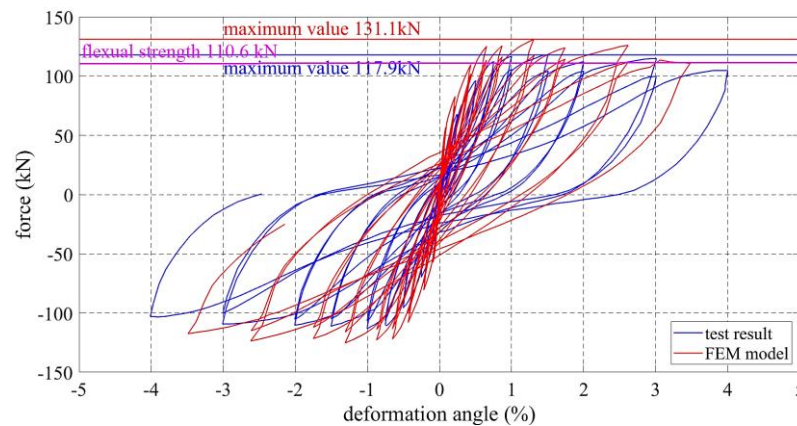

Fig. 6 – Comparison of the force-deformation angle curves results
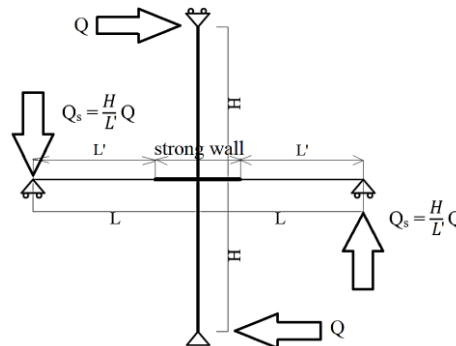

Fig. 7 – Relationship between overall lateral flexural strength and slab flexural force

The lateral flexural strengths calculated from the draft equation, obtained from the experimental test and FEM analysis are 110.6 kN, 117.9 kN and 131.1 kN for the positive deformation range, respectively. The draft equation slightly underestimates whereas the FEM overestimates the flexural strength of this wall-slab joint.

It was observed from Fig. 6 that (i) the hysteretic loops obtained from FEM result larger initial stiffness; (ii) the FEM model also had approximately 11% higher strength than that obtained from the test result; (iii) the hysteretic loops show a reduction on strength after reaching its peak strength for both in FEM and test results; (iv) the FEM loops show a weak lateral deformation comparing with the experimental loops; (v) the hysteretic loops of test result had a greater pinching effect in which the force is smaller when passing through a deformation angle of 0%. The difference in the stiffness, strength, and deformation might be associated to micro-cracks due to shrinkage, the pull-out effect of rebar from concrete or the development of slip crack which are not considered in the simulation. Moreover, the increased pinching effect during the test indicates smaller energy dissipation in the joint. However, despite the difference between test and FEM results, the overall behavior was similar, indicating that the modeling is acceptable and reliable for further study on this type of structural joint.

Figs. 8(a) and (b) present damage pattern at the final stage of the slab upper surface and the bearing wall which obtained from the test and FEM analysis, respectively. It is obvious that cracks including both vertical and diagonal cracks over the surface of the slab and wall observed both in the experiment and FEM analysis. Even though more cracks are observed in the FEM result than that in the test result, the crack pattern obtained from simulation is able to capture the main performance of the crack progressing.

(a)

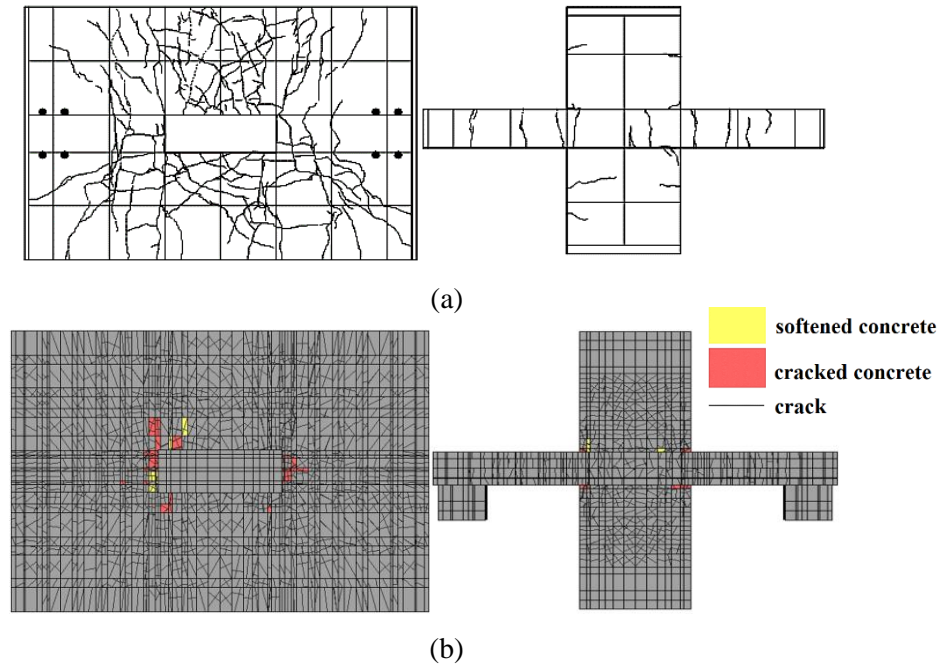softened concrete

cracked concrete

crack

(b)

Fig. 8 – Cracking patterns of the slab upper surface and the bearing wall : (a) test (b) FEM

FEM modeling has been calibrated in this section based on the comparison of force-deformation angle relationship and crack pattern between simulation and test results, indicating that the FEM modeling can be applied to further parametric study.

5. Parametric study

This section presents the numerical results with changing parameters of (i) the wall aspect ratio (height to length), (ii) the slab aspect ratio (length to width), and (iii) the wall axial load on the seismic behavior of the TWTS joint using the calibrated FEM model. In addition, the strengths calculated using the draft equation Eq. (1) mentioned above has been also compared against the numerical analysis results to investigate the accuracy of the equation and influence obtained from different parameters.

5.1 Wall aspect ratio

To investigate the influence of wall aspect ratio on the seismic behavior, five models with different height of wall set at 720 mm, 820 mm, 920 mm, 1020 mm, and 1,120 mm (Fig. 9 (a)) and four models with different wall-length set at 500 mm, 600 mm, 800 mm and 1,000 mm (Fig.9 (b)) were adopted.
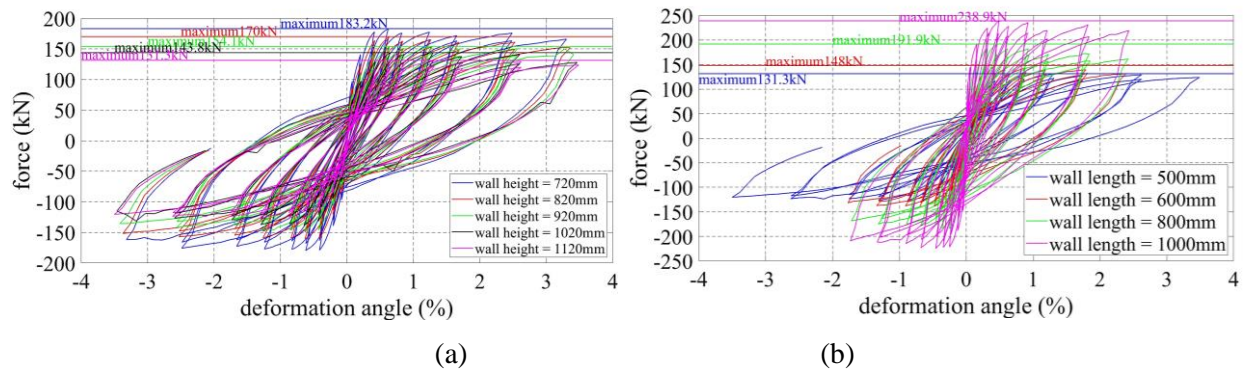

Fig. 9 – (a) Wall height; (b) Wall length

8

(a)   (b)

Fig. 10 – Comparison of the force-deformation angle (a) wall height; (b) wall length

Table 5 – Overall flexural strength values

Wall height	Wall length	Wall aspect ratio (height/ length)	Strength(calculated)	Strength(FEM)
720 mm	500 mm	1.44	171.9 kN	183.2 kN
820 mm	500 mm	1.64	151.0 kN	170.0 kN
920 mm	500 mm	1.84	134.6 kN	154.1 kN
1020 mm	500 mm	2.04	121.4 kN	143.8 kN
1120 mm	500 mm	2.24	110.6 kN	131.3 kN
1120 mm	600 mm	1.87	110.6 kN	148.0 kN
1120 mm	800 mm	1.40	110.6 kN	191.9 kN
1120 mm	1000 mm	1.12	110.6 kN	238.9 kN

Fig. 10 shows comparisons of the force-deformation angle relationship and the peak strengths obtained from the draft equation Eq. (1) mentioned above as well as FEM are shown in Table 5. When the wall height is increased (wall aspect ratio increases), the lateral strength decreases whereas the calculated values are less than the FEM values, which indicates that the draft equation underestimates the flexural strength. When the wall length increases (wall aspect ratio decreases), the strength becomes larger while the calculated value reminds constant. In general, the overall strength decreases as wall aspect ratio increases, either by increasing wall height or decreasing wall length. In addition, the overall strengths are all larger than that calculated using the draft equation by assuming only the " beam element " effective, which indicates that the slab portions which are not connected to the wall directly also bring contribution to the overall capacity and these contributions decrease as wall aspect ratio increases.

5.2 Slab aspect ratio

To investigate the influence of slab aspect ratio on the seismic behavior, six models with the same reinforcement ratio but different width of slab has been set at 350 mm (wall beam that heavily reinforced portion), 675 mm (wall beam that heavily reinforced portion + ordinary slab portion), 850 mm (wall beam that heavily reinforced portion + ordinary slab portion), 1175 mm (wall beam that heavily reinforced portion + ordinary slab portion), 1500 mm (wall beam that heavily reinforced portion + ordinary slab portion), and 1675 mm (wall beam that heavily reinforced portion + ordinary slab portion) as shown in Fig. 11(a) and five models with different length of the slab has been set at 1763 mm, 2163 mm, 2563 mm, 2963 mm and 3363 mm as shown in Fig.11(b) was adopted, respectively.
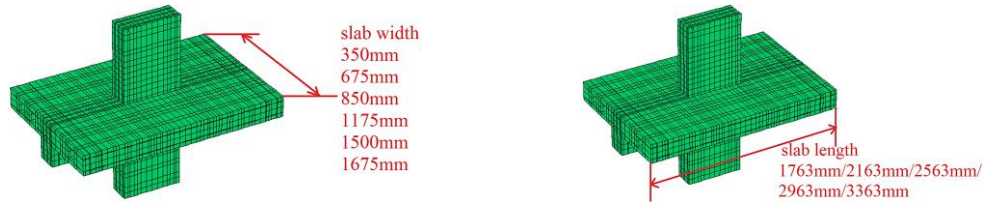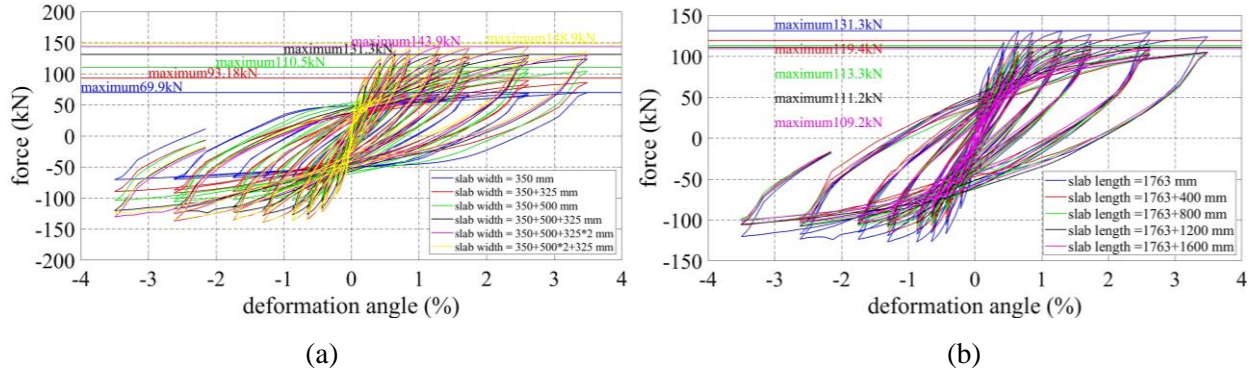
9

Fig. 11 – (a) slab width; (b) slab length

| (a) | (b) |

Fig. 12 – Comparison of the force-deformation angle (a) slab width; (b) slab length

Table 6 – Overall flexural strength values

Slab length	Slab width	Slab aspect ratio (length/ width)	Strength(calculated)	Strength(FEM)
1763 mm	350 mm	5.04	110.6 kN	69.9 kN
1763 mm	675 mm	2.61	110.6 kN	93.18 kN
1763 mm	850 mm	2.07	110.6 kN	110.5 kN
1763 mm	1500 mm	1.18	110.6 kN	143.9 kN
1763 mm	1675 mm	1.05	110.6 kN	148.9 kN
1763 mm	1175 mm	1.50	110.6 kN	131.3 kN
2163 mm	1175 mm	1.84	110.6 kN	119.4 kN
2563 mm	1175 mm	2.18	110.6 kN	113.3 kN
2963 mm	1175 mm	2.52	110.6 kN	111.2 kN
3363 mm	1175 mm	2.86	110.6 kN	109.2 kN

Fig. 12 shows the comparisons of force-deformation angle relationship and Table 6 shows the strengths obtained from FEM analyses. As the slab width increases (i.e. slab aspect ratio decreases), the lateral strength increases from 69.9 kN to 148.9 kN, whereas the strengths which are calculated using the draft equation Eq.(1) by assuming only the "beam element" (heavily reinforced portion of slab) has contributed to the overall strength reminds constant; indicating that the slab width has a positive influence on the overall lateral strength. On the other hand, when the slab length increases (i.e. slab aspect ratio increases), the lateral strength decreased from 131.3 kN to 109.2 kN while the calculated strengths remind the same, which means increasing the slab length has a negative effect on the overall lateral flexural strength. In total, the slab aspect ratio does have an effect on the overall lateral strength, changing the aspect ratio by adjusting slab-width do has a big effect whereas adjusting slab-length cannot bring as much great influence on the overall lateral strength.

10

5.3 Wall axial load

To investigate the influence of axial load applied to the top of the wall on the seismic behavior, five models with different axial load ratios from 0 to 0.4 in steps of 0.1 as shown in Fig. 13 (a) are adopted.
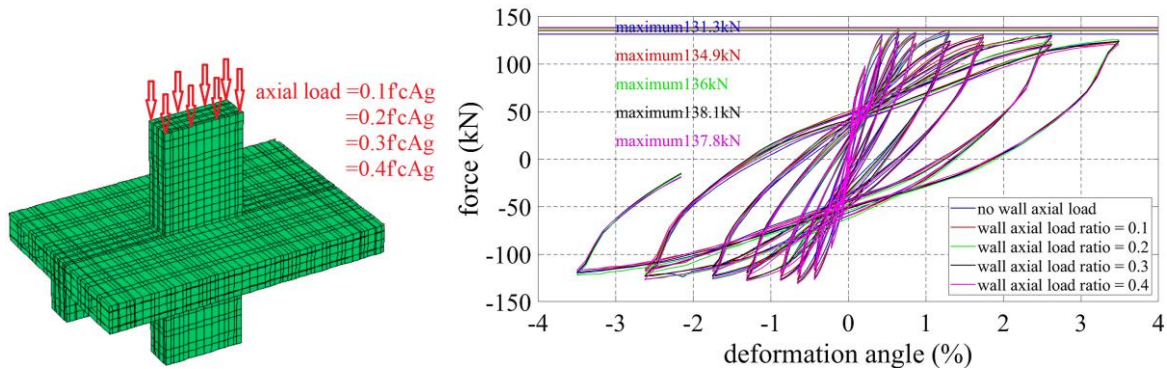

Fig. 13 – (a) axial load on the bearing wall; (b) Comparison of the force-deformation angle

Table 7 – Overall flexural strength values

Axial load ratio (axial load/f'_cA_g)	Strength$_{(calculated)}$	Strength$_{(FEM)}$
0	110.6 kN	131.3 kN
0.1	110.6 kN	134.9 kN
0.2	110.6 kN	136.0 kN
0.3	110.6 kN	138.1 kN
0.4	110.6 kN	137.8 kN

Fig. 13 (b) shows the comparison of force-deformation angle relationship while Table 7 shows the resulting lateral strength. Here, the overall flexural strength increases slightly from 131.3 kN to 137.8 kN and greater than the strength calculated using the draft equation Eq. (1) mentioned above as the axial load increases. Given the relatively small change in strength compared to the change in axial load ratio, the amount of lateral flexural strength increasing is can be ignored.

6. Summary and conclusions

Based on the analyses described in this paper, it can be concluded that:

(1) The FEM analysis is reliable for simulation of the wall-slab joint of thick wall-thick slab structure, and connected material models used in this study can be adopted for further research.

(2) The draft equation underestimates the lateral flexural strength of the thick wall-thick slab joint, and the contribution of the slab portion connected to the "beam element" (heavily reinforced portion of slab) but not connected to the thick wall directly to the overall flexural strength has been confirmed, which indicates that the similar term "effective beam" of slab would be established for the joint of TWTS structure and need further investigations.

(3) As for the lateral flexural strength of wall-slab joint of thick wall-thick slab structure, (i) it decreases with increasing wall aspect ratio (either by increasing wall height or decreasing wall length), (ii) the slab aspect ratio does bring an effect on the lateral strength by changing the slab width, and this effect is considered that the reinforcement in the extra slab portion shows a positive influence on the total lateral strength of the joint whereas the slab aspect ratio by adjusting the slab length doesn't have a major influence on the total lateral

11

strength of the joint; and (iii) adding compressive axial load had minor influence on the overall flexural strength of wall-beam joint.

7. Future direction

Fundamental effects have been investigated for the strength of TWTS joints with regard to wall and slab aspect ratios and axial load ratio. However, the following points can be concerned in future work:

i) A reliable analytical model to predict the lateral strength of the thick wall-thick slab joint of the TWTS structure needs to be established based on the parametric results in this study.

ii) Since the effect of a similar term "effective beam" in the thick wall- thick slab joint as that in flat-plate-floor structure has been confirmed, a detailed procedure to evaluate the "effective beam" needs further investigations.

8. Acknowledgments

9. References

[1] Building Research Institute (1996): Reconnaissance Report of the 1995 Hyogo-kenn Nanbu Earthquake.

[2] National Institute for Land and Infrastructure Management & Building Research Institute (2016): Quick Report of the Field Survey and the Building Damage by the 2016 Kumamoto Earthquake.

[3] Architectural Institute of Japan (2010): AIJ Standard for Structural Calculation of Reinforced Concrete Structures revised 2010, Architectural Institute of Japan.

[4] Architectural Institute of Japan (2015): AIJ Standard for Design and Calculation of Reinforced Concrete Boxed-Shaped Wall Structures, Architectural Institute of Japan.

[5] Kawata Y, Inai E, Akita T, Imagawa N (2017): Loading tests in the in-plain direction of wall-slab joints in box-shaped thick slab and thick wall structures: Part 2 Test results of Specimen 2. *Proceedings of annual research meeting Chugoku Chapter*, (40), 251-254.

[6] Dovich, Laurel M., Wight, James K. (2005): Effective slab width model for seismic analysis of flat slab frames. *ACI Structural Journal*, (102), 868-875.

[7] Obayashi Corporation Technical Research Institute (2018): FINAL – 3D non-linear analysis for concrete structures.

[8] Nakanuma K (1995): Stress-strain Relationship for Concrete under Triaxial Compression. *Transactions of AIJ. Journal of structural and construction engineering*, 60(474) 163-170.

[9] Kupfer,H.B.and Gerstle,K.H. (1973): Behavior of Concrete under Biaxial Stress, *Journal of the Engineering Mechanics Division*, ASCE, Vol.99, No.EM4, pp.853-866.

[10] Nakanuma K (1990): Tension Stiffening Model under In-plane Shear Stress. *Summaries of technical papers of annual meeting Architectural Institute of Japan*, 649-650.

[11] Izumo J (1987): Analytical model for RC plate element subjected to in-plane loading. *Journal of Concrete Research and Technology,* 25(9) 107-120.

[12] Nakanuma K. & Ohkubo M. (2000): An Analytical Model for Reinforced Concrete Panels under cyclic Stresses. *Journal of structural and construction engineering,* (536) 135-142.

[13] Ciampi,V,et al. (1982): Analytical Model for Concrete Anchorages of Reinforcing Bars Under Generalized Excitations. *Report No. UCB/EERC-82/23, Univ. of California, Berkeley (Nov,1982).*

12